

TEM Observation of Reaction at the Interface between Yttria-Doped Ceria and Yttria-Stabilized Zirconia

Hidemi Mitsuyasu, Yasushi Nonaka, Koichi Eguchi,¹ and Hiromichi Arai

Department of Materials Science and Technology, Graduate School of Engineering Sciences, Kyushu University, Kasugakoen, Kasuga, Fukuoka 816, Japan

Received July 1, 1996; in revised form November 11, 1996; accepted November 13, 1996

Interfacial reaction between yttria-stabilized zirconia (YSZ) and yttria-doped ceria (YDC) phases was analyzed by X-ray diffraction and high-resolution transmission electron microscopy. An X-ray diffraction pattern indicated that the mixture of YSZ and YDC consisted of their original phases after heating at 1100°C, whereas a solid state reaction occurred between them at higher temperatures. The solid state reaction proceeded as the Ce component was dissolved into the cubic YSZ phase, with an expense in the amount of the cubic YDC phase. The completion of the reaction gave a single cubic fluorite phase of Y-doped zirconia–ceria (Y CZ) solid solution at 1500°C or high temperatures. A high-resolution transmission electron microscopic analysis supported this reaction process. No solid state reaction was observable at the interface of the ceria and zirconia particles on heating at 1100°C. Although the YDC and YSZ particles are tightly combined at the interface, the lattice kept its original array and orientation. The sample heated at 1300°C contained particles undergoing solid state reaction. The YDC phase was observed in the interface region of the zirconia side. The surface region of Y CZ which faced the ceria particle contained a number of defects. The formation of defects is accompanied by the dissolution of ceria in the zirconia lattice and the lattice of zirconia was distorted to fit to the orientation of the ceria lattice. After heating at 1500°C the sample consisted of a homogeneous Y CZ phase. © 1997 Academic Press

1. INTRODUCTION

Stabilized zirconia has been actively investigated as an oxide ion conductor for application to oxygen sensors, solid oxide fuel cells (SOFC), and the electrochemical oxygen pumps. Yttria-stabilized zirconia has been regarded as the most promising electrolyte for an SOFC, with high conductivity and transference number of the oxide ion. However, the use of this compound at high temperatures around 1000°C is possible. Recently, several investigators have been developing materials for reduced temperature SOFC. Cation-doped ceria has been also investigated as a substitute

for stabilized zirconia, though its reduction in hydrogen atmosphere and resultant electronic conduction is one problem for practical application. We have previously proposed to overcome this difficulty by using a bilayered electrolyte consisting of cation-doped ceria and stabilized zirconia (1, 2). High ionic conductivity of ceria and high resistance in the reducing atmosphere of zirconia are simultaneously attained by adopting this structure. Both stabilized zirconia and doped ceria crystallize in the cubic fluorite structure, whereas their lattice constants are different. The phase diagram of the system $\text{CeO}_2\text{--ZrO}_2\text{--CaO}$ has been reported (3). Two separated fluorite phases of ceria and zirconia stably coexist at low temperatures of ca. 1100°C, but a homogeneous single solid solution of cubic fluorite structure is formed at 1600°C or higher temperatures (4). Other oxide-doped $\text{CeO}_2\text{--ZrO}_2$ systems are expected to follow this basic phase transition behavior, though the stability of each fluorite phase is influenced by the kind of dopants. Yoshimura *et al.* (5–8) have explained phase equilibria in the system $\text{ZrO}_2\text{--CeO}_2$ and established metastable–stable phase diagrams. The transport properties of oxide ion strongly depend on the mixing of cerium and zirconium ions as well as dopant concentration of aliovalent cations such as Ca or Y (9, 10). The dissolution of zirconia in ceria generally results in the deterioration of the ionic conductivity (11, 12). Thus, the interfacial reaction between these two fluorite phases is particularly important for electrochemical applications. The atomic arrangement and defect structure at the interface of these phases are also expected to affect the performance. The purpose of the present study is to analyze structures at the interface between stabilized zirconia and cation-doped ceria using X-ray diffraction and transmission electron microscopy.

2. EXPERIMENTAL

2.1. Sample Preparation

Yttria (Y_2O_3) was selected as a dopant for both ceria and zirconia. Yttria-doped ceria (YDC) with the composition $(\text{YO}_{1.5})_{0.2}(\text{CeO}_2)_{0.8}$ was prepared by thermal

¹ To whom correspondence should be addressed.

decomposition of the corresponding nitrate mixture by heating at 900°C in air. The samples consisted of a single phase of a cubic fluorite structure, as was identified by XRD after sintering. A commercially available yttria-stabilized zirconia (YSZ) was used without further treatment. The composition of YSZ was $(\text{Y}_2\text{O}_3)_{0.08}(\text{ZrO}_2)_{0.92}$ (Tosoh, TZ-8Y). The sample consisted of a single cubic fluorite phase, as was confirmed by XRD. The lattice constants of YDC and YSZ were different, but agreed with the reported values. The powders of ceria and zirconia (molar ratio = 1:1) were mixed together and ball-milled for 24 hr. Then the samples were heated at 1100–1700°C for 5 hr in air.

2.2. X-Ray Diffraction and TEM Observation

The crystalline phase in the sample were identified by X-ray diffraction (XRD) using Rigaku, RINT 1400 with monochromated $\text{CuK}\alpha$ radiation. Silicon and magnesia standards were used for calibration of diffraction angles.

For the observation by a transmission electron microscope (TEM), the preheated powder sample was dispersed in ethanol, and the sample holder with a microgrid was immersed to the dispersion to make the TEM sample. TEM observation was made using JEOL JEM-2000FX with an energy dispersive X-ray analyzer (EDX, Tracor Nothern TN-2000) and JEOL-4000EX for high-resolution observation. The lattice constants were determined by selected area diffraction patterns (SADP), and the camera length was calibrated with single crystalline 10 mol%-YSZ for each observation. In the present study, precise quantitative compositional analyses by EDX were not possible from the following reasons. An electron beam with 50 nm in diameter was employed to derive sufficiently intense of X-ray emission from the samples. Therefore, the EDX data often included the compositional information from the surrounding particles. The intensity of X-ray depended on the thickness of the sample. The thickness was quite different from particle to particle, since fine particles of YDC and coarse particles of YSZ was used in this study. From the similar reasons, compositional distribution of Y species was not evaluated.

3. RESULTS AND DISCUSSION

3.1. Crystalline Phases Determined by X-Ray Diffraction

XRD patterns of the mixture of yttria-doped ceria and yttria-stabilized zirconia after heating treatment at 1100–1700°C are shown in Fig. 1. After heating at 1100°C, the diffraction pattern consisted of the two cubic fluorite phases from ceria and zirconia. Their respective patterns and diffraction angles were the same as those of the samples before the heating treatment. No peak showed shift of the diffraction angle. Therefore, the solid state reaction did not proceed at this heating stage. After heating at 1300°C, the

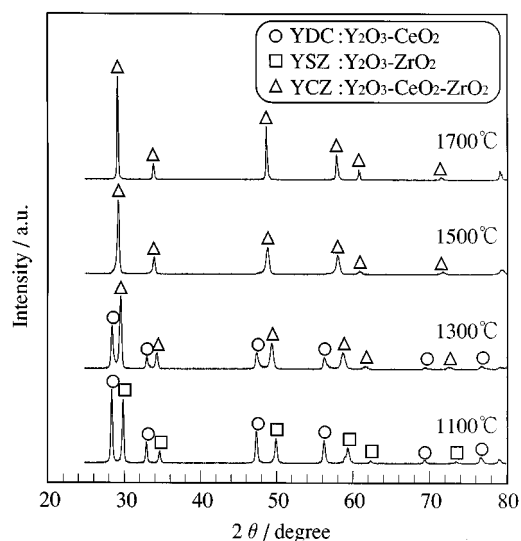


FIG. 1. XRD patterns of mixture of $(\text{YO}_{1.5})_{0.2}(\text{CeO}_2)_{0.8} / (\text{YO}_{1.5})_{0.15}(\text{ZrO}_2)_{0.85}$ (weight ratio = 1/1) after heating at 1100–1700°C for 5 hr.

diffraction lines from the ceria phase was slightly weakend, but the diffraction pattern of this phase and the angles were almost unchanged with the sample before heating. On the other hand, every diffraction line from the zirconia phase slightly shifted to smaller angle than the original position, but the cubic fluorite structure was maintained. After heating at 1500°C, the diffraction lines from the zirconia phase were further shifted to small angles, whereas those from the cubic ceria phase were completely disappeared. This means that the solid state reaction to form the homogeneous solid solution was completed at this temperature. The diffraction pattern was unchanged after heating at higher temperature (1700°C).

The lattice constants of the two fluorite phases after heating treatment are summarized in Table 1. It is conceivable that the Y-doped $\text{Ce}_x\text{Zr}_{1-x}\text{O}_2$ phase is formed through the dissolution of cerium ions into ZrO_2 structure as a solid state reaction proceeds at 1300°C or higher temperatures in the ceria/zirconia sample. This Y-doped $\text{Ce}_x\text{Zr}_{1-x}\text{O}_2$ phase, exhibiting a pattern basically similar to that of the YSZ

TABLE 1
Lattice Constants of Ceria and Zirconia Phases Determined by XRD after Heat Treatment at 1100–1700°C for 5 hr

Temperature/°C	Ceria/Å	Zirconia/Å
1100	5.410	5.144
1300	5.410	5.197
1500	—	5.261
1700	—	5.266

phase except for the systematic shifts of the diffraction angles, is abbreviated as YCZ hereafter. The formation of the YCZ phase accompanies the weakening of the lines from the YDC phase and the shift of the YSZ lines. Only two cubic phases were observable in the present system, since both the original YDC and the YSZ phase contains Y species. The $Ce_xZr_{1-x}O_2$ phase without dopants has been reported by Meriani *et al.* [13] to be tetragonal at small x values. Although yttrium ions should also migrate between the two phases in the present system, the observation was focused on the movement of Ce and Zr ions, since the precise composition analysis was difficult for the Y species.

Detailed observation has been performed for the interfacial reaction and the dissolution of ceria in the zirconia lattice.

3.2. Electron Microscopic Observation

The results of TEM observation after heat treatment at different temperatures are shown in Figs. 2–5. The YDC sample prepared from nitrate and the commercial YSZ powder were used as the source materials for TEM observation. The YDC sample consisted of micrograined polycrystalline particles, whereas the zirconia powder consisted of spherical large particles with a single grain. Such a large

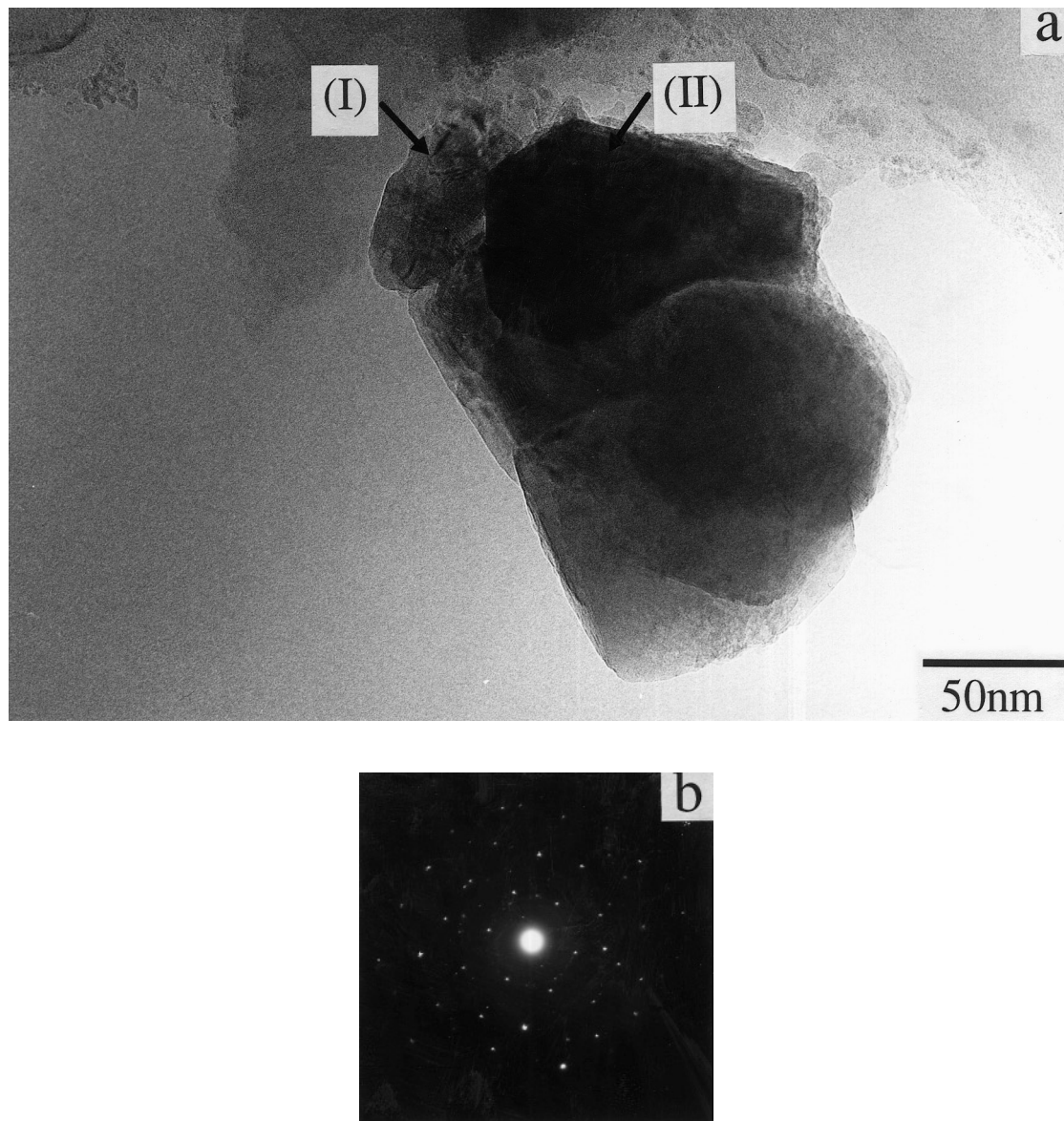


FIG. 2. TEM observation of YDC/YSZ particle interface after heating at 1100°C. (a) TEM image of the particles. (b) Electron diffraction pattern of the particles. (c) High-resolution image of the interface region.

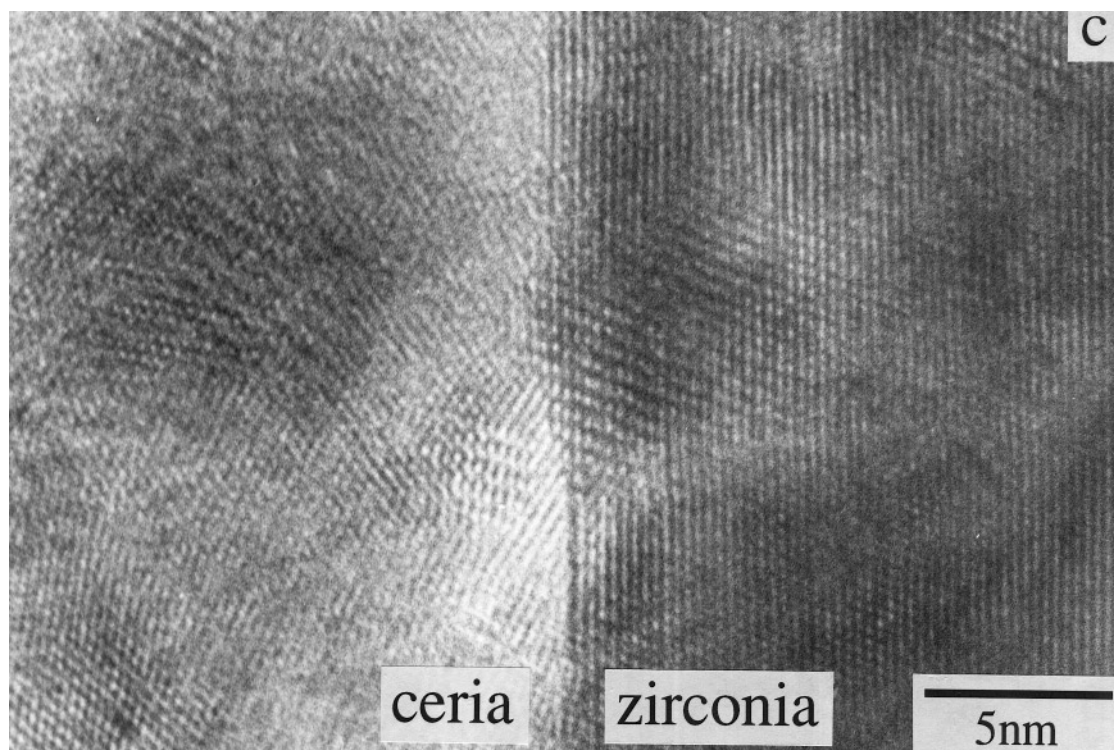


FIG. 2—Continued

microstructural difference enables us to distinguish each particle from the high-resolution images without taking the EDX spectrum for each particle. Therefore, the interface between the two phases can easily be found.

3.2.1. Sample after Heating at 1100°C. The TEM photographs of the sample after heat treatment at 1100°C are shown in Figs. 2a–c. The compositional analyses by EDX at the two different locations (I) and (II) of the particle agglomerate indicated that a large amount of Ce was included in position (I), where a number of thin grains can be seen. On the other hand, the analysis of the thick position (II) showed the existence of Zr, but the Ce component was hardly detected.

The electron diffraction pattern of the YDC/YSZ particle after heating at 1100°C is shown in Fig. 2b. Strong spots from single crystalline YSZ and weak diffraction streaks from polycrystalline YDC were overlapped.

The high resolution image at the interface of the YDC and YSZ grains in this sample is shown in Fig. 2c. A polycrystalline particle of ceria with grain size ca. 3–10 nm exhibited contrasting microstructure with the large-grained zirconia particle (ca. 100 nm). Although the ceria particle consisted of fine grains, the high crystallinity of each grain was obvious from the image. The interface between ceria and zirconia was faceted. Neither distortions nor defects could be found in YDC or YSZ lattices. This microstructure

implies that dissolution between YDC and YSZ did not occur significantly at this heating temperature. This could also be supported from the XRD pattern in Fig. 1. The YDC and YSZ lattices kept their original array even at the atomic layers in the vicinity of the interface. Therefore, no evidence for the solid state reaction was observable from this faceted interface.

3.2.2. Sample after Heating at 1300°C. The TEM observation results for the sample heat-treated at 1300°C are shown in Figs. 3a–d. A ceria particle with a number of small grains exhibits a marked contrast in grain morphology to a large zirconia-based particle with a single grain (Fig. 3a). The EDX analysis indicated that the polycrystalline particle on the left side (I) was abundant in Ce, i.e., the YDC particle. Cerium was also contained in the zirconia-based particle at the right side (II). This means that dissolution of Ce into this zirconia-based particle proceeded significantly to form the YCZ phase. The extent of dissolution was large in the whole particle of YCZ as well as the in the vicinity of interface with the YDC particle.

The electron diffraction pattern of the sample after heating at 1300°C is shown in Fig. 3b. Strong diffraction spots from crystalline YCZ and weak streaks from polycrystalline YDC could be discerned from the pattern. The lattice constant estimated from the strong spot pattern is 5.19 nm, in agreement with that of the YCZ estimated from XRD.

An incident electron beam was introduced along the $[110]$ direction of the YCZ particle after heat treatment at 1300°C to observe the high-resolution lattice image near the interface with YDC. The particle on the right side is YCZ and on the left is the polycrystalline YDC particle. Some stacking faults were observed in the YCZ particle as bright lines along the $[-111]$ direction. This image agrees with the diffraction pattern, in which the spots of the (110) plane from YCZ and the ring from polycrystalline YDC are overlapping. The lattice images for both particles were clearly seen even in the vicinity of the interface. An amorphous grain boundary, which has often been observed for the

interfaces and grain boundaries of covalent crystals, hardly existed for this ionic crystal system. It is noted that the lattice orientation in the interface region of the YCZ particle was different from that in the internal core region. Periodic shadows appeared partly in the interface region of the YCZ particle. This region was ca. 10 nm in width and expanded along the interface region of the zirconia particle as shown in the figure.

The interface region with periodic shadows, which is squared in Fig. 3c, was further magnified in Fig. 3d. The crystal orientation in this interface region of the YCZ part was fit to that of YDC but not the YCZ core, as shown by

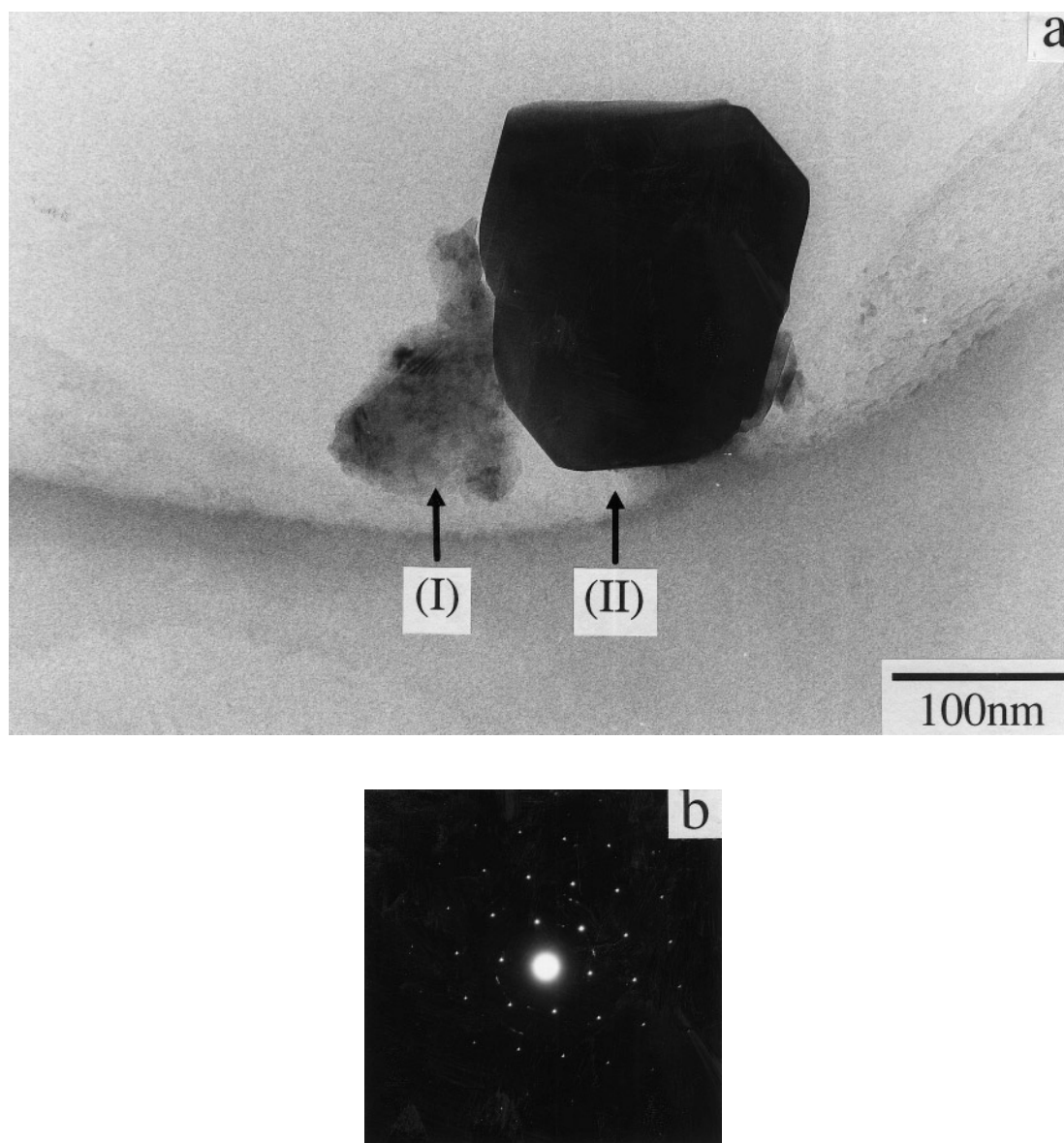


FIG. 3. TEM observation of YDC/YSZ particle interface after heating at 1300°C . (a) TEM image of the particles. (b) Electron diffraction pattern of the particles. (c) High-resolution image of the interface region. (d) Lattice image of the squared region in (c).

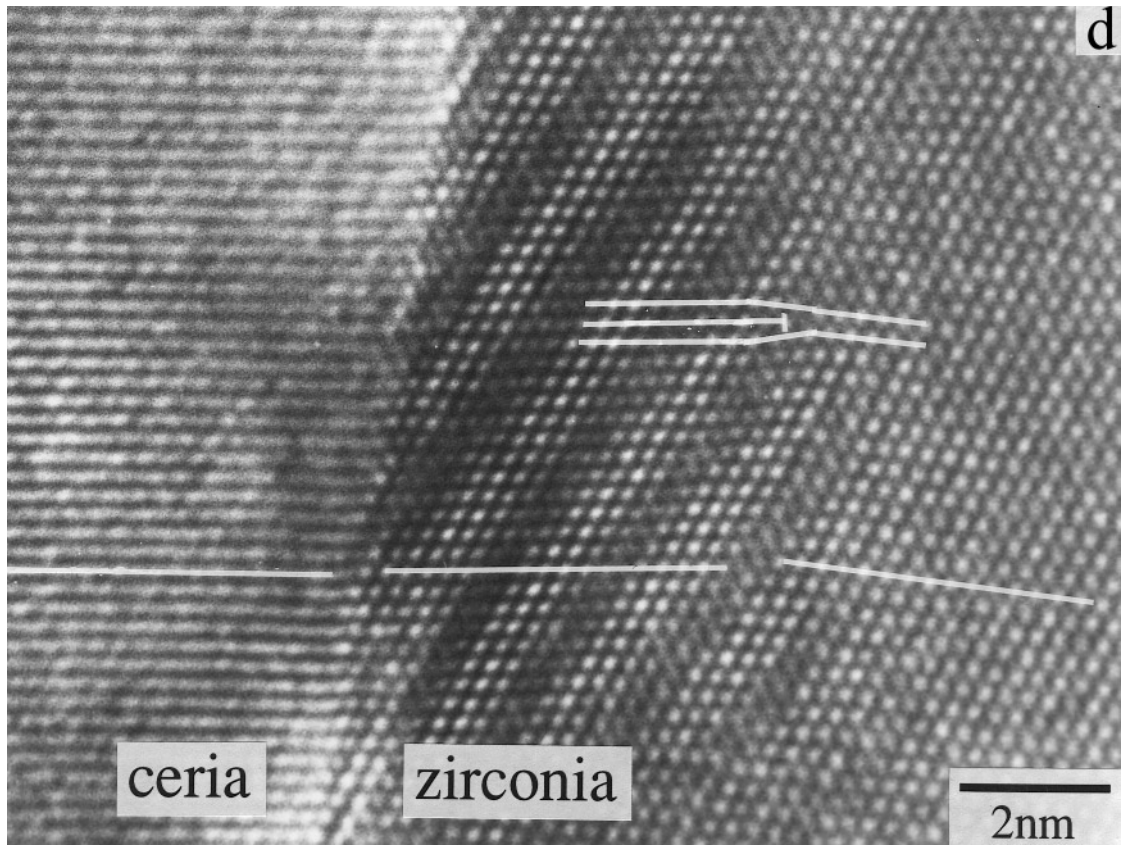
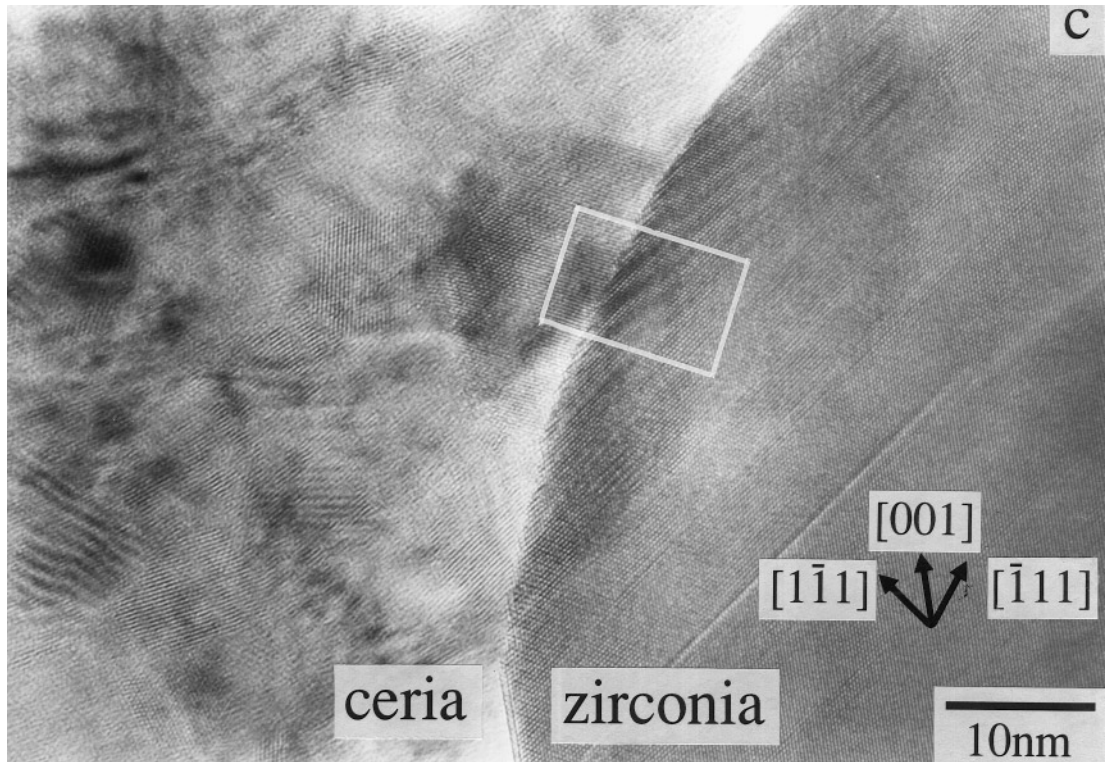


FIG. 3—Continued

the bars in Fig. 3d. A number of dislocations should be introduced to fit the orientation of the interface region of the YCZ shell and the YDC grain. An example was shown in the figure. Obviously the migration of the Ce component affected the crystal orientation of this interface region. The interface region with the shadow stripes possesses a crystal orientation equal to that of YDC. The lattice orientation is different from that of the original YDC in the core region after deformation. The migration of Ce (and Y) into the YSZ or YDC lattice is expected to introduce a number of defects in the interface region. The XRD in Fig. 2 also indicated preferential migration of Ce to the YSZ or YCZ phase, whereas the lattice constant of YDC was unchanged.

3.2.3. Samples after Heating at 1500°C and 1700°C. The high-resolution image of the sample heated at 1500°C is shown in Fig. 4a. The cerium component could be detected by EDX in the whole region of this photograph. However, the fine-grained ceria polycrystal, which was observed for the samples heated at 1100°C and 1300°C, was not observed in this sample. The electron diffraction pattern of this particle is shown in Fig. 4b. Neither diffraction rings nor streaks from a polycrystalline body appeared in the pattern after heating at 1500°C. Disorder and defects of the lattice could hardly be observed either in the high-resolution image or in the diffraction pattern. The lattice constant agreed with that of YCZ observed from the XRD pattern. Thus,

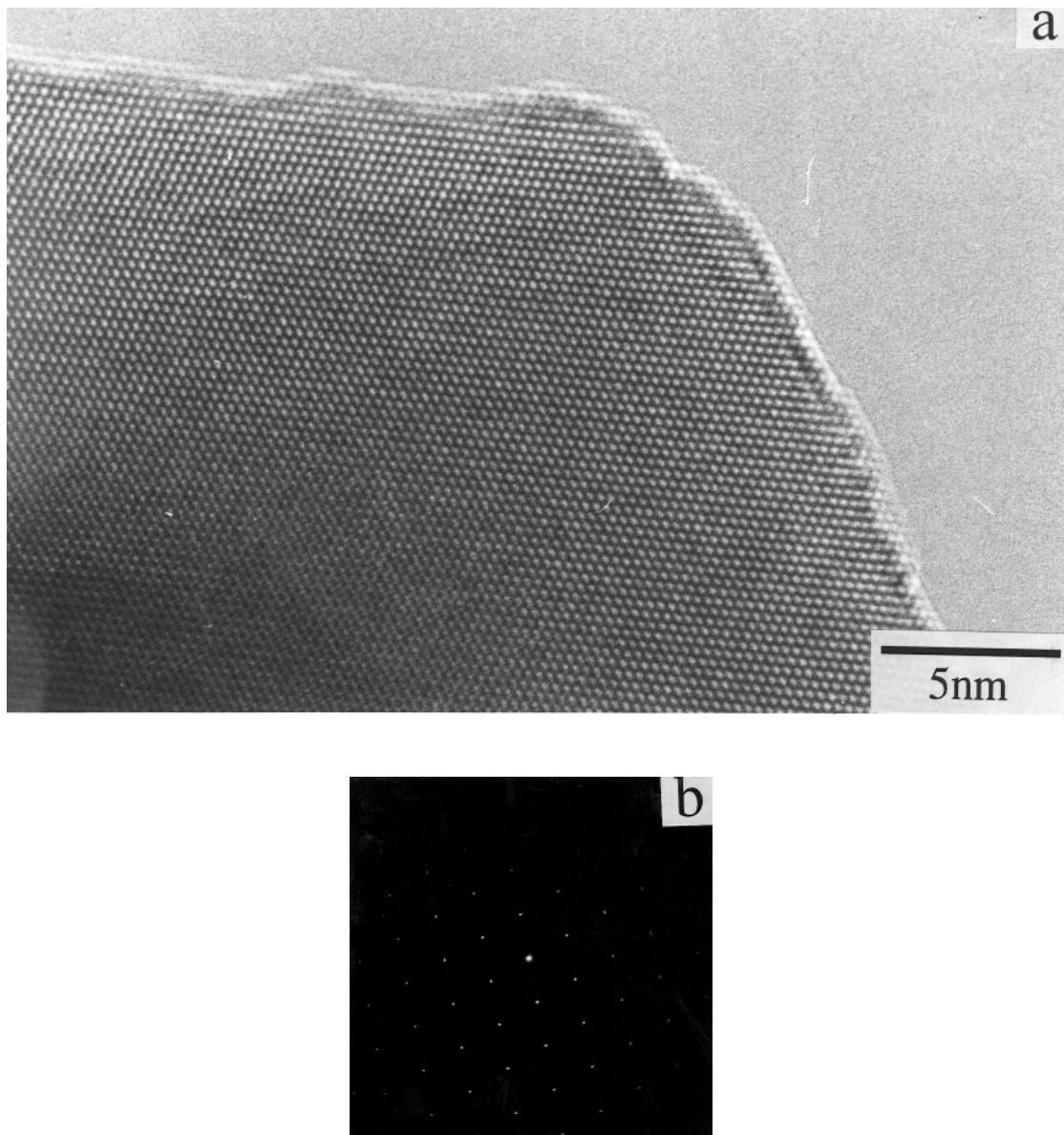


FIG. 4. TEM observation of YCZ particle formed after heating at 1500°C. (a) High-resolution image. (b) Electron diffraction pattern.

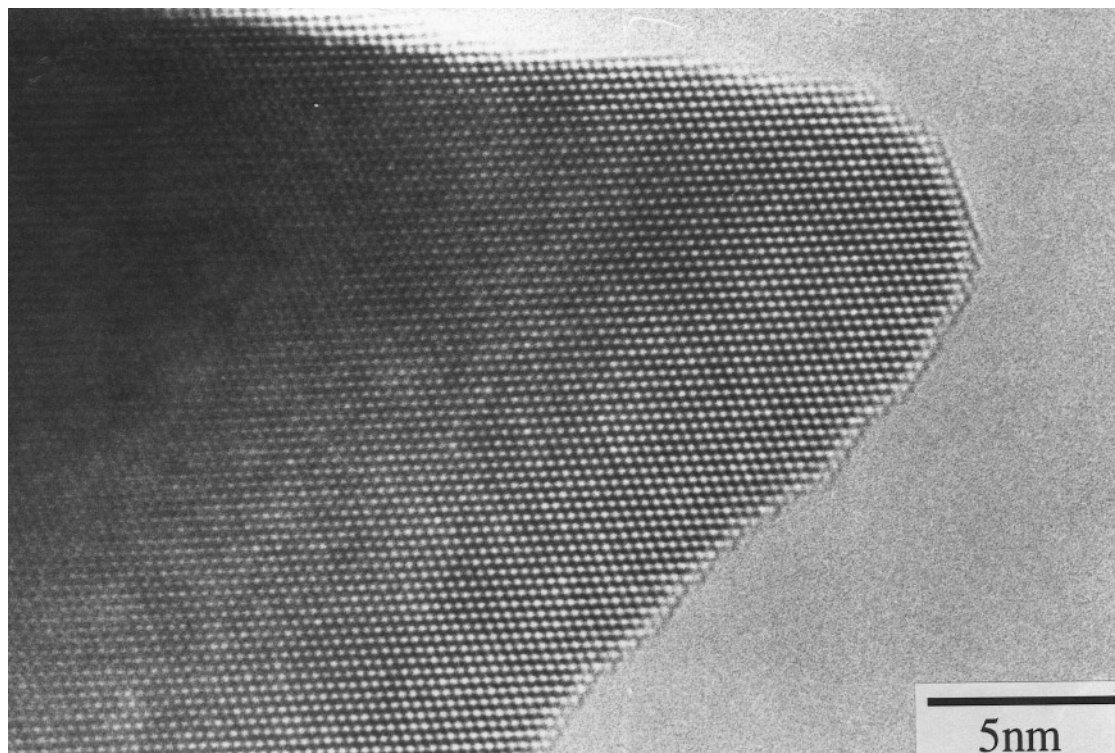


FIG. 5. High-resolution image of YCZ particle after heating at 1700°C.

this sample consists of a homogeneous YCZ particle after complete migration of each component.

The result for the sample heated at 1700°C in Fig. 5 was basically the same as observed for the sample heated at 1500°C. Therefore, at 1500°C or higher temperatures the single solid solution of fluorite YCZ is the sole stable phase.

CONCLUSION

The reaction at the interface between stabilized zirconia and cation-doped ceria has been observed by high-resolution transmission electron microscopy. The interface was basically constructed as the binding of well-crystallized grains even in the vicinity of the interface. The interfacial reaction was observed typically for the sample heated at 1300°C. The reaction starts by the migration of Ce component into the YSZ lattice. The reaction accompanies local deformation and defect formation in the interface region. The reaction was completed at 1500°C or higher temperatures to form the homogeneous single cubic phase. The crystal formed at high temperature is almost defect-free as far as observed by TEM. These reaction processes should be important in understanding the transport properties of the oxide ion in the ceria-zirconia binary ionic conductors system.

ACKNOWLEDGMENT

The present work was partially supported by the Grant-in-Aid for Scientific Research on Priority Areas (No. 260) from the Ministry of Education, Science, Sports, and Culture, Japan.

REFERENCES

1. H. Yahiro, T. Ohuchi, K. Eguchi, and H. Arai, *J. Mater. Sci.* **23**, 1036 (1988).
2. K. Eguchi, T. Setoguchi, T. Inoue, and H. Arai, *Solid State Ionics* **52**, 165 (1992).
3. V. Longo and L. Podda, *Ceramurgia* **1**(2), 83 (1971).
4. Y. Du, M. Yashima, T. Koura, M. Kakihana, M. Yoshimura, *Scripta Metallurg. Material.* **31**(3), 327 (1994).
5. E. Tani, M. Yoshimura, and S. Sōmiya, *J. Am. Ceram. Soc.* **66**(7), 506 (1983).
6. M. Yashima, K. Morimoto, N. Ishizawa, and M. Yoshimura, *J. Am. Ceram. Soc.* **76**(7), 1745 (1993).
7. M. Yashima, H. Takashima, M. Kakihana, and M. Yoshimura, *Rep. Res. Lab. Eng. Mater. Tokyo Inst. Technol.* **19**, 41 (1994).
8. M. Yashima, T. Mitsuhashi, H. Takashima, M. Kakihana, T. Ikegami, and M. Yoshimura, *J. Am. Ceram. Soc.* **78**(8), 2225 (1995).
9. E. C. Subbarao and H. S. Maiti, *Solid State Ionics* **11**, 317 (1984).
10. H. Yahiro, K. Eguchi, and H. Arai, *Solid State Ionic* **36**, 71 (1989).
11. B. Calès and J. F. Baumard, *J. Electrochem. Soc.* **131**, 2407 (1984).
12. C. Leach, N. Khan, B. C. H. Steele, *J. Mater. Sci.* **27**, 3812 (1992).
13. S. Meriani and G. Spinolo, *Powder Diffract. J.* **2**, 255 (1987).